Soft Matter

# Topology Effects on Associative Polymers

| | |
|---|---|
| Journal: | *Soft Matter* |
| Manuscript ID | SM-ART-04-2025-000368.R2 |
| Article Type: | Paper |
| Date Submitted by the Author: | 10-Jun-2025 |
| Complete List of Authors: | Bracewell, John; Clemson University, Dept of Chemistry<br>Sivaraj, Rosita; Clemson University, Dept of Chemistry<br>Perahia, Dvora; Clemson University, Dept of Chemistry<br>Grest, Gary; Sandia National Lab, Center for Integrated Nanotechnology |
| | |

# Topology Effects on Associative Polymers

John C. Bracewell,[1+] Rosita Sivaraj,[1+] Dvora Perahia[1,2*] and Gary S. Grest[3*]

[1]Department of Chemistry, Clemson University, Clemson, South Carolina 29634, USA

[2]Department of Physics, Clemson University, Clemson, South Carolina 29631, USA

[3]Sandia National Laboratories, Albuquerque, New Mexico 87185, USA

+Authors of equal contributions

## Abstract

Tailoring the topology of associative polymers bearing distinctive interacting groups offers potential for formidable landscape of macromolecular responses that will enable design of new responsive materials. The current study probes the conformation, and response of ring associative polymers in comparison with their entangled linear analogues using molecular dynamics simulations of a coarse-grained bead-spring model. The uniqueness of ring polymers lies in their topology where the chains have no free ends, resulting in considerably faster dynamics compared to their linear analogs, whereas the associative groups drive assembly that constrains the polymer motion. Here, polymers consisting of randomly distributed associative groups, with a fraction $f$ = 0.02 to 0.1 and interaction strength varying from 2 to 8 $k_BT$ were studied. We find that with increasing $f$ and association strength, larger clusters of associative groups are formed, where their size and dynamics are strongly affected by chain topology. While the associative groups do not impact the chain conformation, they slow stress relaxation, with a distinctively stronger effect on the linear chains. This is attributed to the lower number of unique chains associated in clusters of the same size in ring melts compared with linear ones. Overall, the coupling of associating groups with entanglements results in slower stress relaxation, where the distinctive topologies affect the association of the chains.

Key Words: Associative Polymers, Ring Polymers, Molecular Dynamics Simulations

# I. Introduction

The unique response of polymers is a compounded function of distinctive chemistries and topologies.[1-3] Among the chemistries that impact polymers are associative whose interaction energies are above van der Waals, such as hydrogen bonds, π–π interactions groups as well as ionizable ones that are often critical to the functionality of these polymers in their many applications. They often drive assembly of the macromolecules that affect their structure and often constrain their motion. Tethering the associating groups (AGs) to chains with distinctive topologies open the way to design new responsive polymers. The delicate balance between chain topology and the constraints exerted by the AGs remains to be determined. It is fundamental to systems that are controlled by two distinctive energy scales and is a key to the function and stability of polymers in current and potential applications.

The topology of chains can be linear, branched, comb or star-like, circular, as well as brush-like. Combined with associative groups, moieties whose interaction energies are typically higher than van der Waals, tethered to their backbone, polymers exhibit markedly diverse characteristics, forming a formidable landscape of macromolecular responses.[4-7] A notable number of studies have focused on either the effects of topology[8-12] or associative groups on polymer structure, dynamics, and response but none have examined the combined effect of topology and associating groups.

Only limited experimental studies probe the correlations between polymer topology, among which are polymer brushes, where only one end is free where the other is confined. In these systems, the electrostatic environment strongly affects chain conformation and in turn affect the mechanical response of these systems.[13, 14]

Associative ring polymers and loopy segments, are prevalent in nature, where for example, topology-associated groups correlations affect protein folding as well as assembly of DNA into networks[15] and is critical in understanding assembly into chromatin.[16-18] In these bio systems, specific association of amino acids coupled with topology dictates the ability of the chains to assemble. In the realm of synthetic polymers, the conjunction of topology and associative groups offer a design tool for macromolecular response. The interrelation between the topology and the impact of associative groups, however, remains a convoluted uncharted territory with hardly any experimental studies.

Here, using a coarse grain bead-spring model, we probe using molecular dynamics simulations[19, 20] the structure, chain mobility and mechanical response of ring AG decorated polymers in comparison with their linear analogue as the strength of the associative polymers is varied. We find that topology affects the number of chains that constitute each of the clusters, determining the response of the polymers.

Ring polymers are distinguished by the simple fact that they lack free ends, affecting their structure and dynamics.[12, 21] Linear chains in a melt assume a Gaussian conformation with their size scaling as $N^{1/2}$, where $N$ is the degree of polymerization.[2] The topological constraint of no free ends force ring polymers to form globularly compact structures whose size scales as $N^{1/3}$.[12] Ring polymers are less entangled compared with linear chains with similar N, resulting in higher mobility. The motion of rings proceeds as loops of increasing size rearrange progressively where linear polymers dynamics is constrained by entanglements.[22, 23] The enhanced dynamics that stem from the topology of the molecules expresses itself in a much faster stress-relaxation in ring compared to linear chains melts.[24-26]

The correlation of topology effects with presence of AGs presents a challenge given that addition of even a small fraction of interacting associating groups to the polymer backbone,

dramatically changes the properties of the system and drive assembly.[4-7] These AGs either form pairwise associations, such as hydrogen bonds, or larger directional assemblies, such as π–π stacks, or clusters such as ionizable groups.[7] The latter exhibit long range interactions that drive collective assemblies to form ionic clusters.[27-29] The size, shape, and lifetime of these clusters all affect the structure and dynamics of the chains. The current work seeks to resolve the interrelation between associating groups in rings compared with linear entangled polymers.

The unique dynamics of associative polymers and their technological potential have driven significant efforts including various computational studies using both fully atomistic simulations of model polymers such as polystyrene sulfonate, and coarse-grained chains, each providing insight into distinctive length scale. Using fully atomistic models, Agrawal et al.[30] have shown that for polystyrene sulfonate, increasing the dielectric constant of the media, which reduces the strength of the ionic interaction between associating $SO_3^-$ groups, decreases the size of the ionic cluster and enhances the dynamics. Mohottalalage et al.[31] have shown that the distribution of ionic groups along the polymer backbone affects the size and shapes of these ionizable groups and their dynamics. Studies of segmental motion by Frischknecht et al.[32] and Winey and Frischknecht[33] on precise poly(ethylene-co-acrylic acid) ionomers showed that the local motion of the chains slows down as clusters are formed. They showed that the ionic aggregates form various shapes ranging from isolated aggregates to percolated aggregates depending on the separation of the space length. Paren et al.[34] found that the ionic groups on precise single-ion conductors, consisting of a polyethylene backbone with sulfonated phenyl pendant groups, nanophase separate from the polymer backbone to form percolating ionic aggregates. Using a coarse grained bead spring model, Hall et al.[35, 36] embedded charged beads and studied their effects on the structure. Sadeghi et al.[37] extended this model to study polyampholyte ionomers in which both types of ions are incorporated in the polymer chain and

compared their dynamics and structures with the conventional cationic ionomers, where only cations are incorporated into the polymer chain.

With the realization that topology plays a significant role, Senanayake et al.[38] studied the effect of the strength of the associating groups on chain mobility and viscoelastic response of melts of unentangled linear chains and star polymers. They found that for a 3-arm star polymer melt, the average size of the assemblies remains as for a linear polymer melt of the same molecular weight. However, the number of unique chains associated with each cluster is smaller for the associative star melt compared with the linear chain melt.

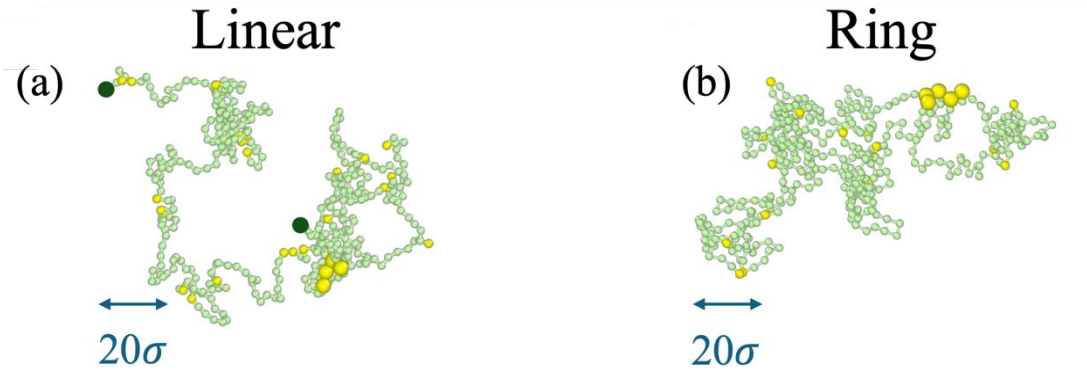


Figure 1: Visualizations of an individual linear and ring chain for $f = 0.05$ with strength of the associating bead interactions of 5 $k_BT$. Each chain contains 400 beads. The associating beads (yellow) are increased in size for clarity.

To understand the effect of chain topology on the assembly process of associating groups, we use molecular dynamics (MD) simulations of a coarse-grained bead spring model in which the interacting groups are incorporated in the form of associating beads randomly distributed along the backbone.[38] We compare the structure, chain mobility, and stress relaxation for entangled linear chain melts with ring polymer melts of the same chain length.

Specifically, we study a range of associating group interactions from 2 to 10 $k_BT$ for associating group fractions of $f = 0.02$ to 0.10. Experimentally, changing the associated group interaction

would entail changing the chemistry of the association group. The lower interaction range is characteristic of co-polymers where the interactions of minority species are stronger than those of the majority component. With increasing interactions, the model captures the association of AGs, such as those present in non-ionic surfactants, and the higher interactions typical to ionizable groups, all driving collective assembly. A visualization of a linear and a ring chain with associative beads extracted from ring and linear melts is shown in Figure 1.

Similar to melts of non-associative polymers, the linear chains are more extended compared with the rings. The conformational difference between individual ring and linear chains in non-associative polymers is attributed to the nature of confinement of the macromolecules. The extended conformation of the linear chains arises from their confinement to a tube of their neighbors where the ends move more freely. Rings, however, do not have free ends, and are thus more globular. As the strength of attraction between the associating groups and their concentration increases, the size of the clusters of associating beads increases, leading to long lived, transient networks, in both linear and ring melts.

## II. Model and Methodology

The Kremer–Grest coarse-grained model[19, 20] with beads of mass $m$ and diameter $\sigma$ connected by finite extensible nonlinear elastic (FENE) bonds was used to compare the structure and dynamics of associating polymer melts of linear and ring polymers. Non-connected beads interact with a Lennard-Jones potential,

$$U_{\alpha\beta}(r) = \begin{cases} 4\varepsilon_{\alpha\beta}\left(\left(\frac{\sigma}{r}\right)^{12} - \left(\frac{\sigma}{r}\right)^{6}\right) & r \leq r_c \\ 0 & r > r_c \end{cases} \qquad (1)$$

where the cutoff $r_{cut} = 2.5\,\sigma$ for all beads. The chains contain two types of beads, non-associating beads (type 1), which interact with strength $\varepsilon_{11}$ and associating beads (type 2), which interact

with strength $\varepsilon_{22} > \varepsilon_{11}$. The cross term $\varepsilon_{12} = \varepsilon_{11}$. The ratio of the interaction strengths $\varepsilon_s = \varepsilon_{22}/\varepsilon_{11}$ was varied from 1 to 8, which captures the interaction energies of random copolymers to ionic interaction energies. The fraction of random associating beads $f$ = 0.02, 0.05 and 0.10. This range of associating bead strength and concentration is sufficient to qualitatively affect the size of clusters of associating groups and reduce chain mobility.

All simulations are carried out using the Large Scale Atomic Molecular Massively Parallel Simulator (LAMMPS) software.[39] Melts of linear chains of 400 chains of length $N$ = 400 were prepared following the procedure described by Auhl et al.[40] Ring melts of 1600 chains of length $N$ = 400 were prepared following the procedure developed by Smrek et al.[41] The equations of motion were integrated with a time step at $\Delta t = 0.01\tau$, where $\tau = (m\sigma^2/\varepsilon_{11})^{1/2}$ is the standard time unit for a Lennard-Jones fluid, where $m$ is the mass of the bead. The beads are coupled to a Langevin thermostat to maintain the temperature T = $\varepsilon_{11}/k_B$ with a damping time constant of $10\tau$.[42, 43] The glass transition $T_g \sim 0.48\varepsilon_{11}/k_B$ for a linear, homopolymer melt with no associating beads.[44] The beads are connected by FENE bonds with a spring constant $K = 30\ \varepsilon_{11}$ and $R_0 = 1.5\sigma$. The polymers are semiflexible with a 3-body cosine angle interaction $V_{angle}(\theta) = k_\theta[1 + cos(\theta)]$ with $k_\theta = 1.5\varepsilon$. The entanglement length $N_e \sim 28$ for linear chains for this model.[45, 46] Thus, for the linear chain melts studied here, the number of entanglements per chain $Z = N/N_e \sim 14$. Following equilibration with no associating groups, a fraction $f$ of the beads in the systems were randomly changed to associating beads, type 2. The evolution of the associating groups was then followed as a function of time for $\varepsilon_s = 2 - 8$ at constant pressure. After the density and average cluster size of the associating groups reached a steady state, the systems were run at constant volume for 3-4 x $10^7$ $\tau$. The number density of each system is $\rho \approx 0.89\text{-}0.92\sigma^{-3}$, depending on value of the associating bead strength $\varepsilon_s$ and fraction $f$. The measured radius of

gyration of the chains is found to be independent of the fraction and strength of the associating beads as shown in Figure S1.

The static structure factor *S(q)* for the associating beads is calculated by

$$S(q) = \frac{\sum_{i,j=1}^{N} b_i b_j \langle exq[i\boldsymbol{q}\bullet(\boldsymbol{r}_i - \boldsymbol{r}_j)]\rangle}{\sum_{i=1}^{N} b_i^2},$$

where $b_i$ is the scattering length density for monomer $i$. Due to the periodic boundary conditions, the wavevector $\boldsymbol{q}$ is limited to $\boldsymbol{q} = \frac{2\pi}{L}(n_x, n_y, n_z)$, where $L$ is the simulation cell length and $n_x$, $n_y$, and $n_z$ are integers. The scattering length density is set to $b_i = 1$ for associating beads and to $b_i = 0$ for non-associating beads.

## III. Structure of Linear and Ring Melts

The assembly process of associating groups was followed over time with varying the

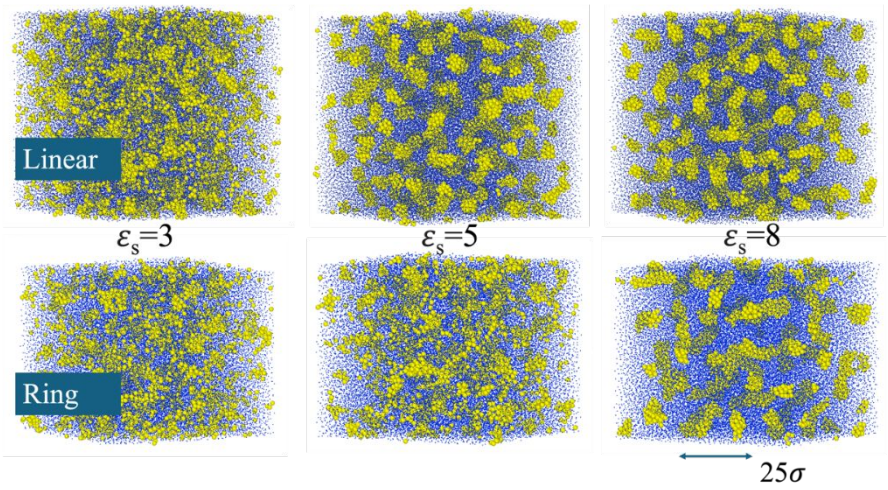


Figure 2. Visualization of a section of the melts of linear and ring chains for $f$=0.05 after the systems have reached steady state. The associating beads are yellow, and the non-interacting beads are blue. The associating beads are increased in size for clarity.

interactions strength $\varepsilon_s$ and associating bead fraction $f$. The visualization of a section of the ring and linear melts for $f$ = 0.05 for three values of $\varepsilon_s$ is shown in Figure 2. Similar illustrations for $\varepsilon_s$ = 5 for varying $f$ are shown in Figure S1. With increasing $\varepsilon_s$ the AGs assemble to form clusters that become significantly more defined at higher interactions.

The cluster evolution is shown in Figure 3a for $f = 0.05$. Associating groups are defined to reside in the same cluster if they are within 1.5 σ of each other. This distance was chosen to capture all the nearest neighbor pairs as shown in Figure S2 for the pair correlation function between associating bead $g_{aa}(r)$. Similar trends are found for $f = 0.02$ and 0.10. For low association strength, $\varepsilon_s = 2$-4, the average cluster size reaches its final value almost instantly. For $\varepsilon_s \geq 5$, the average cluster size initially rapidly increases with time as nearby associating groups form clusters and then continue to slowly grow, reaching a plateau only at later times. The average cluster size $<N_c>$ at the plateau is presented in Figure 3b as a function of $\varepsilon_s$ for $f =$ 0.02, 0.05 and 0.1. With increasing $\varepsilon_s$, the final average cluster size first increases and then decreases. With increasing $\varepsilon_s$, the energy barrier for the clusters to rearrange increases and the system becomes kinetically trapped. For large $\varepsilon_s$, the associating beads are locked in which ever cluster they first associate with and the cluster size does not change. At lower $\varepsilon_s$, the associating beads can exchange between clusters, resulting in an increase in cluster size compared to large $\varepsilon_s$. Except for the smallest association strength $\varepsilon_s$, $<N_c>$ for the rings is larger than for the linear chains with the largest difference for intermediate interaction strength between AG $\varepsilon_s \sim 5$.

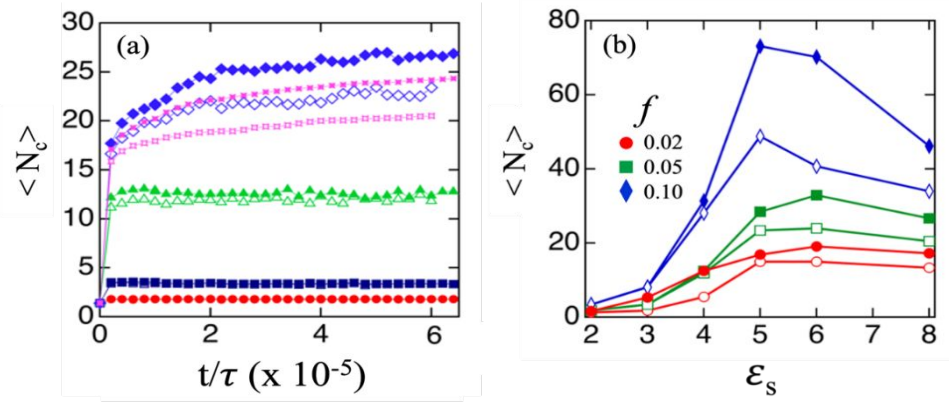


Figure 3. (a) Average cluster size $<N_c>$ as a function of time for linear chains (open) and rings (closed) in polymer melts for $f = 0.05$ at $\varepsilon_s = 2$ (circles), $\varepsilon_s = 3$ (squares), $\varepsilon_s = 4$ (triangles), $\varepsilon_s = 5$ (diamonds), $\varepsilon_s = 8$ (stars). (b) Average cluster size $<N_c>$ for $f = 0.02$, 0.05, and 0.10, at the end of the simulation as a function of association strength $\varepsilon_s$ for linear (open) and ring (filled) polymer chains.

The formation of the AG clusters does not affect the overall dimensions of the chains. The

measured radius of gyration of the chains is found to be independent of the fraction and strength of the associating beads as shown in Figure S3 for both the ring and linear melts. This is presumably because the AG do not move very far to assemble into clusters, in which case the overall dimensions of the chain are not affected.

The mesoscopic correlations in both melts were studied through calculating the static structure factor *S(q)* of the associating beads. The results are shown in Figure 4, where the calculated static structure factor is normalized to the number of beads. For both linear and ring melts, the patterns consist of two distinct features, one at low $q$, which reflects correlations between the associative clusters, and another at high $q$ that corresponds to the packing of the associating beads. At $\varepsilon_s$ =2, there is hardly any signature in the low $q$ regime, as most AGs are not in clusters for both linear and ring melts. As $\varepsilon_s$ increases, the intensity of both the low $q$ peak and AG packing signature increases, and their width decreases.

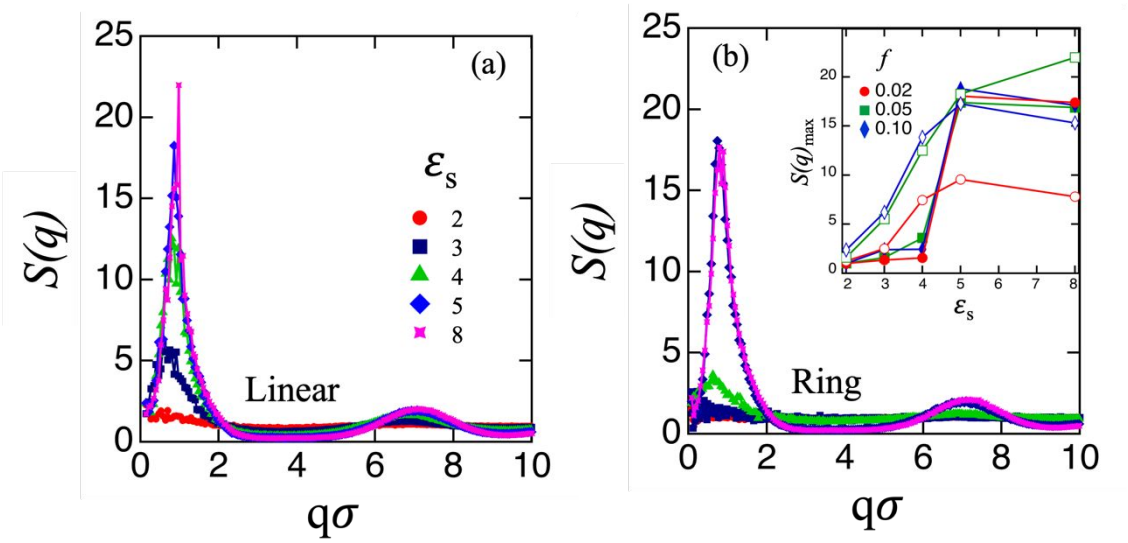


Figure 4. (a) Static structure factor *S(q)* of the associating groups as a function of $q$ for (a) linear chains and (b) rings at the indicated values of $\varepsilon_s$ for $f$ = 0.05. Intensity for the low q peak for *S(q)* as a function of association strength $\varepsilon_s$ for linear (open) and ring (filled) polymer melts is shown in the inset.

Experimentally, the intensity of any peak in a scattering pattern corresponds to the number of objects that contribute to a given signature and its width is inversely proportional to the degree of correlation. Here as *S(q)* is normalized to the number of the associating beads, both the intensities and peak widths reflect the degree of correlation. The insert captures the peak intensity as a function $\varepsilon_s$ for the values of *f* studied. For linear chains, both the intensity and width of the low *q* peak gradually increase with increasing $\varepsilon_s$ and then levels off. For rings the intensity of the low q peak exhibits an abrupt increase between $\varepsilon_s$ = 4 and 5 following by a plateau. At low and intermediate $\varepsilon_s$, the intensity of the low q signature increases with increasing $\varepsilon_s$. At higher $\varepsilon_s$, the peak intensity decreases for all systems except linear chains at *f* = 0.05. The *f* = 0.05, as the systems become kinetically trapped, as shown in the next section, the clusters are most likely not completely equilibrated. Linear chains exhibit higher peak intensities than rings at low and intermediate $\varepsilon_s$. The larger peak intensity for linear chains compared to the rings indicates more well-defined inter-cluster distances, as shown in the visualization in Figure 2.

Cluster formations comprise of associating groups that could belong to different polymers, defined as *unique chains*, or reside on the same chain. The number of unique polymer chains associated with each cluster, along with the cluster's size and shape, significantly impacts the overall dynamics of the melts. Figure 5 presents the average number of unique chains $<N_{uc}>$ in a cluster as a function of cluster size $N_c$. For both the linear and ring melts, $<N_{uc}>$ is independent of the AG strength $\varepsilon_s$ for a given cluster size. For the smallest clusters at low interaction strengths, associations are primarily interchain, with $<N_{uc}> \approx N_c$. As the cluster size grows, $<N_{uc}>/N_c$ decreases, as the number of intra chain associations in the same cluster grows. For a given cluster size, $<N_{uc}>$ is significantly larger for the linear chains compared to the rings as each cluster contains more inter-chain associating groups. This difference is presumably because the rings are much more compact $(<R_g^2>^{1/2} = 7.2\ \sigma)$ than the linear chains (13.3 $\sigma$).

This is also manifested in the fact that the largest cluster size for the rings is larger than for the linear chain melts.

## III. Dynamics and Viscoelastic Response

Association groups constantly break and reform clusters over time. To obtain an insight into the lifetime of the clusters, we measured the survival time of pairs of associating beads that remain in the same cluster as a function of time. This is calculated by first identifying all pairs of associating beads that are within the same cluster and following the number of pairs that remain in the same cluster as a function of time.

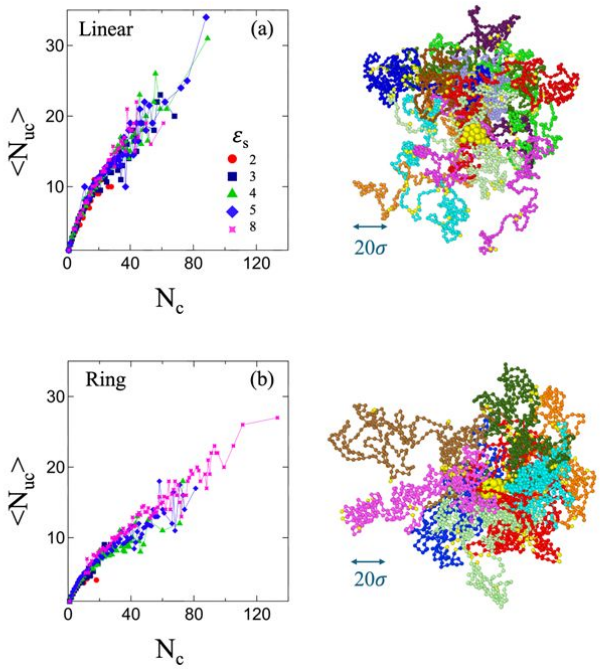


Figure 5. Average number of unique chains $<N_{uc}>$ in a cluster of size $N_c$ as a function of cluster size for linear chains (a) and rings (b) for $f = 0.05$ for the indicated $\varepsilon_s$ values. Visualizations of an average size cluster of associative groups in a melt of linear chains and rings for $f = 0.05$ with associating bead strength of 5 $k_BT$. Each chain contains 400 beads and is marked by different colors. The associated beads are yellow and are increased in size for clarity for the highlighted cluster, which has 23 associating beads in each case. There 11 unique chains for the linear chains and 8 for the rings.

The number of such pairs *Npair(t)* that remain in the same cluster as a function of time is shown in Figure 6. *Npair(t)* decreases either by single associating beads leaving the cluster or the cluster breaking into two or more smaller clusters. Although for the present systems, the decay is predominantly by an associating bead leaving the cluster.

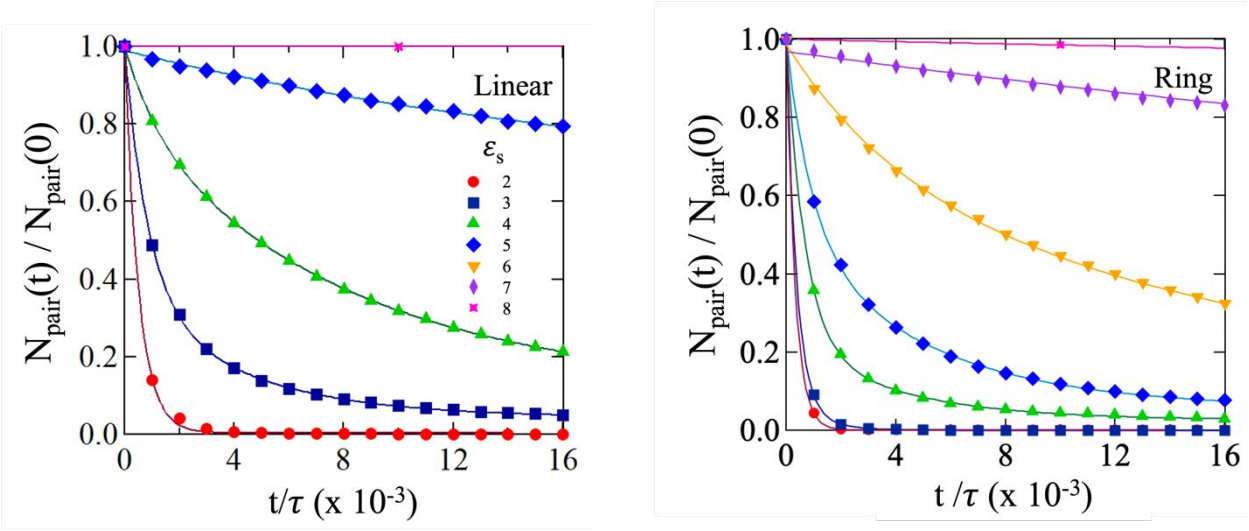


Figure 6. Number of pairs *Npair(t)* that remain in the same cluster as a function of time for a) linear and b) ring melts with $f = 0.05$ for the indicated $\varepsilon_s$ values. The solid lines are fits to a sum of two exponentials.

The results for $N_{pair}(t)$ are fit to the sum of two exponentials,

$$N_{pair}(t)/N_{pair}(0) = A_1 e^{-t/\tau_1} + A_2 e^{-t/\tau_2},$$

where $\tau_i$ are the relaxation times ($\tau_1 > \tau_2$) and $A_i$ are the weighting functions for the two contributions. The sum was constrained in the fit so that $A_1 + A_2 = 1$. Results for $\tau_i$ are shown in Figure 7 and the values of $\tau_i$ and $A_i$ are tabulated in Tables S1 and S2 in the SI. For low association strength $\varepsilon_s$, *Npair(t)* for both the linear and ring melts decay quickly as the associating clusters are small and very dynamic and as a result have minimal effect on the long-time mobility of the chains. As $\varepsilon_s$ increases, the decay times for *Npair(t)* increases rapidly, with

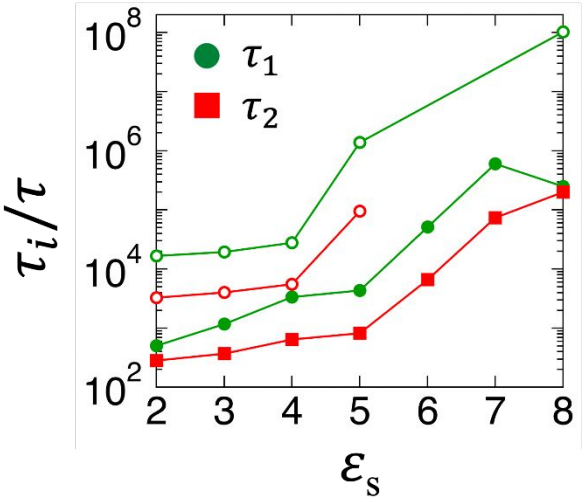


Figure 7. Relaxation times $\tau_i$ as a function of association strength $\varepsilon_s$ for linear chains (open) and rings (filled).

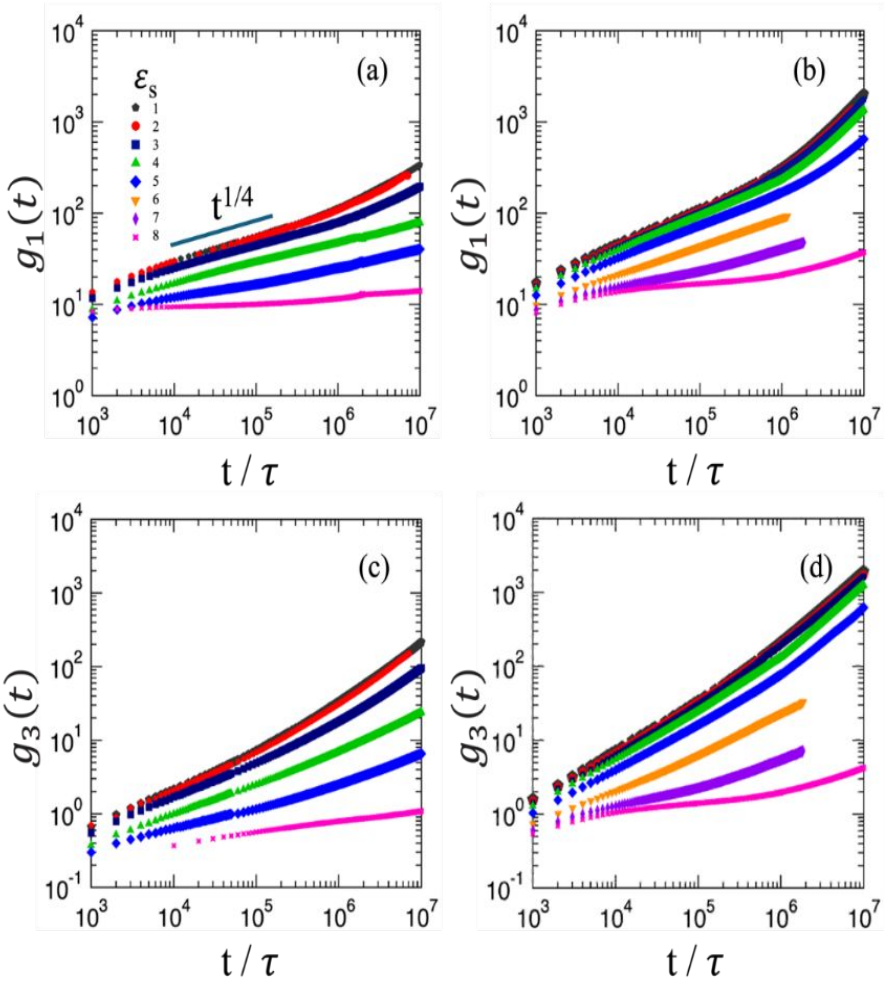


Figure 8. Mean square displacement, $g_1(t)$ of the beads for (a) linear chains and (b) rings as a function of time and for the center of mass (COM) $g_3(t)$ for (c) linear chains and (d) rings for $f = 0.05$ for the indicated $\varepsilon_s$ values.

the decay time always being longer for the linear chains compared to the rings, as the linear

chains are more entangled than the rings. For associating strength $\varepsilon_s$ = 8, the clusters are kinetically trapped. For large $\varepsilon_s$, these long-lived clusters constrain the mesoscopic mobility of the polymer, as is shown in Figure 8.

As the mesoscopic dynamics is coupled to the lifetime of the clusters, we measured the mean squared displacement (MSD) of the monomers $g_1(t) = <(r_i(t) - r_i(0))^2>$ and of the center of mass (COM) $g_3(t)$ of polymer chains. For the linear chains $g_1(t)$ was averaged over the inner 50 beads of the chain, while for the rings, $g_1(t)$ was averaged over all the monomers of the chain. Results for $g_1(t)$ and $g_3(t)$ are presented in Figure 8 for the linear and ring chains for $f$ = 0.05 for different strengths $\varepsilon_s$.

For small associating group strength, $\varepsilon_s < 4$, the mobility of beads in the linear chains presented in Figure 8a, show the characteristic crossover from Rouse scaling $t^{1/2}$ at early times to reptation scaling $t^{1/4}$ at intermediate times at crossover time $\tau_e \sim 2800\ \tau$. At much later times a crossover to the diffusive regime, $g_3(t) \sim t$ is observed for times greater than the diffusive time $\tau_d$. For $N$ = 400 with $\varepsilon_s$=1, $\tau_d = 2.6x10^7\tau$, is determined as the time for the inner beads to move $3<R_g^2>$. For $\varepsilon_s$ = 2, which would model a random copolymer, $\tau_d$ is unchanged for $f$ = 0.02 and increases slightly to $\tau_d = 2.8x10^7\tau$ for $f$ = 0.05 and to $\tau_d = 3.9\ x10^7$ for $f$ = 0.10. For larger $\varepsilon_s$, $g_1(t)$ does not reach the diffusive regime within the time scales currently accessible as the associating groups act effectively as crosslinks.

As the interaction between associating groups increases, mobility of the beads, even at short distances, becomes significantly suppressed, with an effective power law smaller than ¼ expected for reptation. This suppression in the chain mobility is seen very clearly in the mobility of the center of mass $g_3(t)$, shown in Figure 8c. The mobility of the beads for the ring polymers are shown in Figure 8b. For ring melts with no associating groups, Halverson et al.[47] observed a significant slowing down in the mean-square displacement from the initial $t^{1/2}$ scaling to a power law very close to the $t^{1/4}$ expected for reptation of linear polymers, even though rings cannot entangle in the classical sense.[23] As for the linear chains, this behavior is largely unchanged for $\varepsilon_s \leq 4$ for $f = 0.05$ as shown in Figure 8b. Only for larger $\varepsilon_s$, do the associating group begin to dominate the chain mobility. For $f = 0.05$, the diffusive time $\tau_d = 2.4 \times 10^5 \tau$ for $\varepsilon_s = 1$ and 2 and increases only slightly to $\tau_d = 2.5 \times 10^5 \tau$ for $\varepsilon_s = 3$, then starts to increase more rapidly with increasing associating strength, $\tau_d = 3.6 \times 10^5 \tau$ for $\varepsilon_s = 4$ and $\tau_d = 8.0 \times 10^5 \tau$ for $\varepsilon_s = 5$, and $\tau_d = 6.0 \times 10^6 \tau$ for $\varepsilon_s = 6$. For larger $\varepsilon_s$, values, the diffusive regime is beyond the accessible time scales. Similar results are observed for $f = 0.02$ and 0.10. Similar effects of increasing $\varepsilon_s$ on the overall chain mobility are shown in Figure 8d for the motion of the COM of the rings.

These linear and ring melts constitute heterogeneous media where the AG beads form distinctive domains whose dynamics controls the macroscopic motion of the chains and their mechanical response. The mobility of the molecules affects the mechanical response of the system as reflected in the stress relaxation *G(t)* after a small perturbation, which is a prevalent experimental measure of polymer rheology. The stress relaxation is measured using the Green−Kubo relation $G(t)=(V/k_BT)\langle\sigma_{\alpha\beta}(t)\sigma_{\alpha\beta}(0)\rangle$, where $\sigma_{\alpha\beta}(t)$ are the off-diagonal components xy, xz, and yz of the stress and V is the volume of the system. The results are shown in Figure 9 and 10 for linear and ring melts.

For entangled non-associative linear polymers, at short times, *G(t)* decays as the chains locally relax in response to the perturbation. At intermediate times beyond the entanglement time $\tau_e$, *G(t)* plateaus at $G_N^0 = \frac{4\rho k_B T}{5} \frac{}{N_e}$, before decaying to zero after the chains have reached the diffusive regime at $\tau_d$. The results for non-associating melts are in agreement with those of Hsu and Kremer[20] who observed a well-defined plateau at intermediate times for *G(t)* with $N_e$ = 28 for a range of chain lengths. For $\varepsilon_s < 3$, we observe little effect on the stress relaxation for $f$=0.05 as shown in Figure 9a. For larger $\varepsilon_s$, the stress relaxes slower and decays only for very long times. The effect of varying the concentration of associating beads is shown in Figure 9b for $\varepsilon_s = 5$. Increasing the fraction of associating beads has a strong effect on the stress relaxation.

The stress relaxes significantly faster in ring melts than in linear ones. For intermediate chain lengths where the rings do not entangle, the fractal loopy globular model[23] predicts that *G(t)* decay as $t^{-3/7}$, in agreement with the MD simulations of Halverson et al. and Tu et al.[48] For very high molecular weight rings, recent experiments and simulations show non-power-law stress relaxation as the rings interpenetrate.[48]

For $\varepsilon_s < 3$, we observe little effect on the stress relaxation for $f$=0.05 as shown in Figure 9a. For larger for $\varepsilon_s$, the stress relaxes slower and decays only for very long times. The combination of entanglements and strongly interacting associating groups dramatically increases the plateau modulus, consistent with what one finds for crosslinked networks.[49-51] The effect of varying the concentration of associating beads is shown in Figure 9b for $\varepsilon_s = 5$. Increasing the fraction of associating beads retards the stress relaxation and increases the plateau modulus.

For rings, the relaxation times are much faster than for linear chains of the same length as shown in Figure 10. Measurable deviations from the expected $t^{-3/7}$ power law in $G(t)$ occur for $\varepsilon_s \geq 6$

for $f$ = 0.05 and $\varepsilon_s \geq 5$ for $f$ =0.10, although except for the highest AG strength, $G(t)$ is still reasonably well described by a power law, albeit with a smaller amplitude exponent.

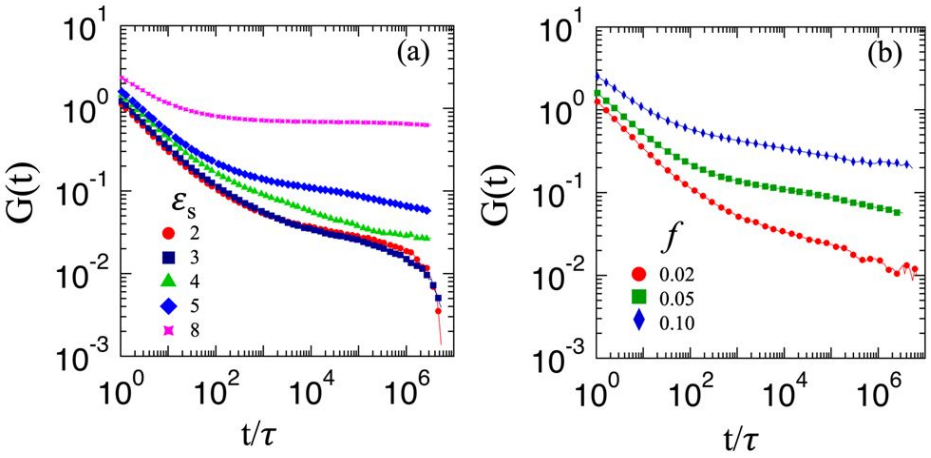


Figure 9. Stress autocorrelation $G(t)$ for linear chains as a function of time at $f$ = 0.05 for the indicated $\varepsilon_s$ values. (b) $G(t)$ for $\varepsilon_s$ = 5 for $f$ = 0.02, 0.05 and 0.10.

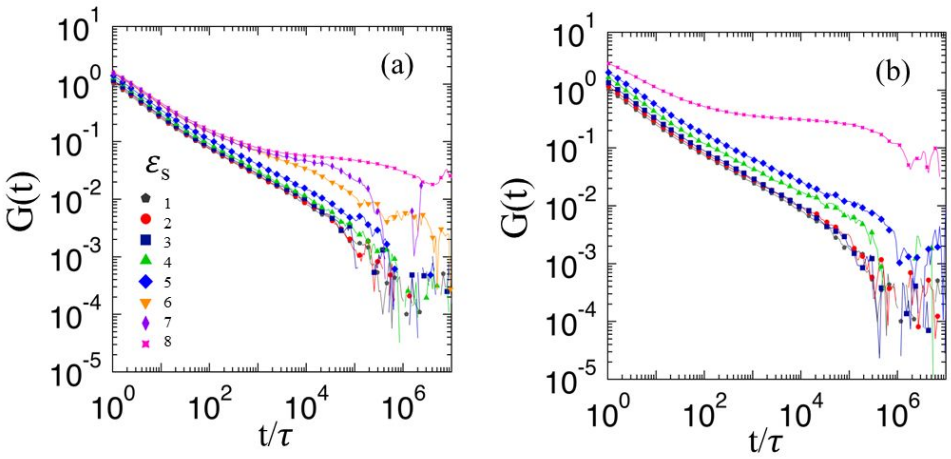


Figure 10. Stress autocorrelation $G(t)$ for ring polymer melts as a function of time for (a) $f$ = 0.05 and (b) $f$ = 0.10 for the indicated $\varepsilon_s$ values.

Though both linear and ring melts reach a plateau for large $\varepsilon_s$, its magnitude is significantly different where the one for the linear systems are high. This is attributed to the lock-in of entanglements by the AGs that do not occur in the ring melts.

## IV. Conclusions

The structure, dynamics and response of ring associative polymer melts were studied in comparison with those of linear melts. Although for both melts the associating beads form clusters with increasing interaction strength between the associate beads, the topology of the polymer affects the nature, size, and stability of the associative domains and hence, their stress relaxation. The clusters for the linear chains form at lower association strength compared with rings and exhibit a narrower distribution. The lifetime of a pair of associating groups in a melt of ring polymers is shorter than that in linear melts.

The linear and ring melt response to stress is distinctive. In linear chains the AGs lock the entanglements, increasing the plateau moduli, which is similar to a crosslinked network. For ring melts with weakly interacting associating groups, the stress relaxes as a power law with an exponent that is smaller in magnitude compared to rings without associating groups. At high $\varepsilon_s$ the stress relaxation exhibits a plateau.

These simulations show that combining topology and associating groups can lead to interesting new phenomena and can be used a design tool for new materials.

Supplemental Information

Visualization of a section of the melts of linear and ring chains for $\varepsilon_s = 5$ for $f = 0.02$, 0.05 and 0.10 together with graphs for the pair correlation function, $g_{aa}(r)$ for the associating bead, and root mean squared radius of gyration as a function of association strength $\varepsilon_s$ are presented in the SI. Tables with the fitting parameters $\tau_i$ and $A_i$ are also given in the SI.

ACKNOWLEDGMENTS

D.P. gratefully acknowledges the financial support given by NSF Grant No. DMR-1905407. This research used in part resources on Palmetto Cluster at Clemson University under NSF awards MRI 1228312, II NEW 1405767, MRI 1725573, and MRI 2018069. This research used resources at the National Energy Research Scientific Computing Center (NERSC), a U.S.

Department of Energy Office of Science user facility, operated under Contract No. DE-AC02-05CH11231. This work was performed, in part, at the Center for Integrated Nanotechnologies, a U.S. Department of Energy and Office of Basic Energy Sciences user facility. Sandia National Laboratories is a multimission laboratory managed and operated by the National Technology and Engineering Solutions of Sandia LLC, a wholly owned subsidiary of Honeywell International Inc., for the U.S. Department of Energy's National Nuclear Security Administration under Contract No. DE-NA0003525. This paper describes objective technical results and analysis. Any subjective views or opinions that might be expressed in the paper do not necessarily represent the views of the U.S. NSF, DOE or the U.S. Government.

* Corresponding authors: dperahi@g.clemson.edu and gsgrest@sandia.gov

References

(1) Roovers, J. *Branched polymers II*; Springer Science 1998.
(2) Rubinstein, M.; Colby, H. R. *Polymer Physics*; Oxford University Press, 2003.
(3) Graessley, W. W. *Polymeric liquids and networks*; Garland Science, 2003.
(4) Rubinstein, M.; Semenov, A. N. Thermoreversible gelation in solutions of associating polymers. 2. Linear dynamics. *Macromolecules* **1998**, *31*, 1386-1397.
(5) Rubinstein, M.; Semenov, A. N. Dynamics of entangled solutions of associating polymers. *Macromolecules* **2001**, *34*, 1058-1068.
(6) Tonge, S.; Tighe, B. Responsive hydrophobically associating polymers: a review of structure and properties. *Adv. Drug Delivery Rev.* **2001**, *53*, 109-122.
(7) Van Ruymbeke, E. Preface: Special issue on associating polymers. *J. Rheo.* **2017**, *61*, 1099-1102.
(8) Klein, J. Dynamics of entangled linear, branched, and cyclic polymers. *Macromolecules* **1986**, *19*, 105-118.
(9) McLeish, T. C. B.; Milner, S. T. Entangled Dynamics and Melt Flow of Branched Polymers. In *Branched Polymers II*, Roovers, J. Ed.; Springer Berlin Heidelberg, 1999; pp 195-256.
(10) Snijkers, F.; Pasquino, R.; Olmsted, P.; Vlassopoulos, D. Perspectives on the viscoelasticity and flow behavior of entangled linear and branched polymers. *J. Phys. Condensed Matter* **2015**, *27*, 473002.
(11) Haque, F. M.; Grayson, S. M. The synthesis, properties and potential applications of cyclic polymers. *Nature Chem.* **2020**, *12*, 433-444.
(12) Kruteva, M.; Allgaier, J.; Richter, D. Topology matters: Conformation and microscopic dynamics of ring polymers. *Macromolecules* **2023**, *56*, 7203-7229.
(13) Raviv, U.; Giasson, S.; Kampf, N.; Gohy, J.-F.; Jérôme, R.; Klein, J. Normal and frictional forces between surfaces bearing polyelectrolyte brushes. *Langmuir* **2008**, *24*, 8678-8687.
(14) Smook, L. A.; de Beer, S. Molecular Design Strategies to Enhance the Electroresponse of Polyelectrolyte Brushes: Effects of Charge Fraction and Chain Length Dispersity. *Macromolecules* **2025**.
(15) Michieletto, D. Kinetoplast DNA: a polymer physicist's topological Olympic dream. *Nucleic Acids Research* **2025**, *53*, gkae1206.
(16) Craik, D. J. Seamless proteins tie up their loose ends. *Science* **2006**, *311*, 1563-1564.

(17) Halverson, J. D.; Smrek, J.; Kremer, K.; Grosberg, A. Y. From a melt of rings to chromosome territories: the role of topological constraints in genome folding. *Rep. Prog. Phys.* **2014**, *77*, 022601.
(18) Chan, B.; Rubinstein, M. Theory of chromatin organization maintained by active loop extrusion. *Proc. Nat. Acad. Sci.* **2023**, *120*, e2222078120.
(19) Kremer, K.; Grest, G. S. Dynamics of entangled linear polymer melts: A molecular-dynamics simulation. *J. Chem. Phys.* **1990**, *92*, 5057-5086.
(20) Hsu, H.-P.; Kremer, K. Static and dynamic properties of large polymer melts in equilibrium. *J. Chem. Phys.* **2016**, *144*, 154907.
(21) Chen, C.; Weil, T. Cyclic polymers: synthesis, characteristics, and emerging applications. *Nanoscale Horizons* **2022**, *7*, 1121-1135.
(22) Grosberg, A. Y. Annealed lattice animal model and Flory theory for the melt of non-concatenated rings: towards the physics of crumpling. *Soft Matter* **2014**, *10*, 560-565.
(23) Ge, T.; Panyukov, S.; Rubinstein, M. Self-similar conformations and dynamics in entangled melts and solutions of nonconcatenated ring polymers. *Macromolecules* **2016**, *49*, 708-722.
(24) Kapnistos, M.; Lang, M.; Vlassopoulos, D.; Pyckhout-Hintzen, W.; Richter, D.; Cho, D.; Chang, T.; Rubinstein, M. Unexpected power-law stress relaxation of entangled ring polymers. *Nature Materials* **2008**, *7*, 997-1002.
(25) Parisi, D.; Costanzo, S.; Jeong, Y.; Ahn, J.; Chang, T.; Vlassopoulos, D.; Halverson, J. D.; Kremer, K.; Ge, T.; Rubinstein, M. Nonlinear Shear Rheology of Entangled Polymer Rings. *Macromolecules* **2021**, *54*, 2811-2827.
(26) Peponaki, K.; Tsalikis, D. G.; Patelis, N.; Sakellariou, G.; Chang, T.; Vlassopoulos, D. Revisiting the viscosity of moderately entangled ring polymer melts. *Macromolecules* **2024**, *57*, 7263-7269.
(27) Eisenberg, A.; Hird, B.; Moore, R. B. A new multiplet-cluster model for the morphology of random ionomers. *Macromolecules* **1990**, *23*, 4098-4107, 10.1021/ma00220a012. DOI: 10.1021/ma00220a012.
(28) Grady, B. P. Review and critical analysis of the morphology of random ionomers across many length scales. *Polymer Eng. Sci.* **2008**, *48*, 1029-1051.
(29) Potaufeux, J.-E.; Odent, J.; Notta-Cuvier, D.; Lauro, F.; Raquez, J.-M. A comprehensive review of the structures and properties of ionic polymeric materials. *Polymer Chem.* **2020**, *11*, 5914-5936.
(30) Agrawal, A.; Perahia, D.; Grest, G. S. Clustering effects in ionic polymers: Molecular dynamics simulations. *Phys. Rev. E* **2015**, *92*, 022601. From NLM PubMed-not-MEDLINE.
(31) Mohottalalage, S. S.; Aryal, D.; Thurston, B. A.; Grest, G. S.; Perahia, D. Effects of Ionic Group Distribution on the Structure and Dynamics of Amorphous Polymer Melts. *Macromolecules* **2021**, *55*, 217-223. DOI: 10.1021/acs.macromol.1c02141.
(32) Frischknecht, A. L.; Paren, B. A.; Middleton, L. R.; Koski, J. P.; Tarver, J. D.; Tyagi, M.; Soles, C. L.; Winey, K. I. Chain and Ion Dynamics in Precise Polyethylene Ionomers. *Macromolecules* **2019**, *52*, 7939-7950. DOI: 10.1021/acs.macromol.9b01712.
(33) Frischknecht, A. L.; Winey, K. I. The evolution of acidic and ionic aggregates in ionomers during microsecond simulations. *J. Chem. Phys.* **2019**, *150*, 064901.
(34) Paren, B. A.; Thurston, B. A.; Neary, W. J.; Kendrick, A.; Kennemur, J. G.; Stevens, M. J.; Frischknecht, A. L.; Winey, K. I. Percolated Ionic Aggregate Morphologies and Decoupled Ion Transport in Precise Sulfonated Polymers Synthesized by Ring-Opening Metathesis Polymerization. *Macromolecules* **2020**, *53*, 8960-8973.
(35) Hall, L. M.; Seitz, M. E.; Winey, K. I.; Opper, K. L.; Wagener, K. B.; Stevens, M. J.; Frischknecht, A. L. Ionic Aggregate Structure in Ionomer Melts: Effect of Molecular Architecture on Aggregates and the Ionomer Peak. *J. Am. Chem. Soc.* **2012**, *134*, 574.

(36) Hall, L. M.; Stevens, M. J.; Frischknecht, A. L. Dynamics of Model Ionomer Melts of Various Architectures. *Macromolecules* **2012**, *45*, 8097.
(37) Sadeghi, N.; Kim, J.; Cavicchi, K. A.; Khabaz, F. Microscopic Morphology and Dynamics of Polyampholyte and Cationic Ionomers. *Macromolecules* **2024**, *57*, 3937-3948.
(38) Senanayake, M.; Perahia, D.; Grest, G. S. Effects of interaction strength of associating groups on linear and star polymer dynamics. *J. Chem. Phys.* **2021**, *154*, 074903.
(39) Thompson, A. P.; Aktulga, H. M.; Berger, R.; Bolintineanu, D. S.; Brown, W. M.; Crozier, P. S.; in't Veld, P. J.; Kohlmeyer, A.; Moore, S. G.; Nguyen, T. D. LAMMPS-A flexible simulation tool for particle-based materials modeling at the atomic, meso, and continuum scales. *Comp. Phys. Comm.* **2022**, *271*, 108171.
(40) Auhl, R.; Everaers, R.; Grest, G. S.; Kremer, K.; Plimpton, S. J. Equilibration of long chain polymer melts in computer simulations. *J.Chem.Phys.* **2003**, *119*, 12718-12728. DOI: .
(41) Smrek, J.; Kremer, K.; Rosa, A. Threading of Unconcatenated Ring Polymers at High Concentrations: Double-Folded vs Time-Equilibrated Structures. *ACS Macro Lett* **2019**, *8*, 155-160.
(42) Schneider, T.; Stoll, E. Molecular-dynamics study of a three-dimensional one-component model for distortive phase transitions. *Phys.Rev.B.* **1978**, *17*, 1302-1322.
(43) Grest, G. S.; Kremer, K. Molecular dynamics simulation for polymers in the presence of a heat bath. *Phys. Rev. A* . **1986**, *33*, 3628-3631.
(44) Grest, G. S. Communication: Polymer entanglement dynamics: Role of attractive interactions. *J.Chem.Phys.* **2016**, *145*.
(45) Sukumaran, S. K.; Grest, G. S.; Kremer, K.; Everaers, R. Identifying the primitive path mesh in entangled polymer liquids. *J. Polym. Sci., Part B:Polym. Phys.* **2005**, *43*, 917-933.
(46) Hoy, R. S.; Foteinopoulou, K.; Kröger, M. Topological analysis of polymeric melts: Chain-length effects and fast-converging estimators for entanglement length. *Phy.Rev.E* **2009**, *80*, 031803.
(47) Halverson, J. D.; Lee, W. B.; Grest, G. S.; Grosberg, A. Y.; Kremer, K. Molecular Dynamics Simulation Study of Nonconcatenated Ring Polymers in a Melt. Ii. Dynamics. *J. Chem. Phys.* **2011**, *134*, 204905.
(48) Tu, M. Q.; Davydovich, O.; Mei, B.; Singh, P. K.; Grest, G. S.; Schweizer, K. S.; O'Connor, T. C.; Schroeder, C. M. Unexpected slow relaxation dynamics in pure ring polymers arise from intermolecular interactions. *ACS Polymers Au* **2023**, *3*, 307-317.
(49) Danielsen, S. P.; Beech, H. K.; Wang, S.; El-Zaatari, B. M.; Wang, X.; Sapir, L.; Ouchi, T.; Wang, Z.; Johnson, P. N.; Hu, Y. Molecular characterization of polymer networks. *Chem. Rev.* **2021**, *121*, 5042-5092.
(50) Wang, J.; O'Connor, T. C.; Grest, G. S.; Ge, T. Superstretchable Elastomer from Cross-linked Ring Polymers. *Phys. Rev. Lett.* **2022**, *128*, 237801.
(51) Dobrynin, A. V.; Tian, Y.; Jacobs, M.; Nikitina, E. A.; Ivanov, D. A.; Maw, M.; Vashahi, F.; Sheiko, S. S. Forensics of polymer networks. *Nature Mat.* **2023**, *22*, 1394-1400.

The trajectories from the molecular dynamics simulations and resulting analysis are available from one of corresponding authors upon request.